Description of Global-Scale Circulation Cells in the Tropics with a 40–50 Day Period

ROLAND A. MADDEN AND PAUL R. JULIAN

National Center for Atmospheric Research,[1] *Boulder, Colo. 80302*

(Manuscript received 6 April, in revised form 15 May 1972)

ABSTRACT

Long time series (5–10 years) of station pressure and upper air data from stations located in the tropics are subjected to spectral and cross-spectral analysis to investigate the spatial extent of a previously detected oscillation in various variables with a period range of 40–50 days. In addition, time series of station pressure from two tropical stations for the 1890's are examined and indicate that the oscillation is a stationary feature. The cross-spectral analysis suggests that the oscillation is of global scale but restricted to the tropics: it possesses features of an eastward-moving wave whose characteristics change with time. A mean wave disturbance, constructed with data from the IGY, provides additional descriptive material on the spatial and temporal behavior of the oscillation. The manifestation in station pressure consists of anomalies which appear between 10N and 10S in the Indian Ocean region and propagate eastward to the Eastern Pacific. Zonal winds participate in the oscillation and, in general, are out-of-phase between the upper and lower troposphere. Mixing ratios and temperatures are also investigated. The sum total of evidence indicates that the oscillation is the result of an eastward movement of large-scale circulation cells oriented in the equatorial (zonal) plane.

1. Introduction

Spectral analysis of 10 years (1957–67) of daily rawinsonde data for Canton Island (3S, 172W) has revealed fairly broad but significant peaks in the station pressure spectrum, in the low tropospheric zonal wind spectrum, and in the upper tropospheric zonal wind spectrum in the 40–50 day period range (Madden and Julian, 1971).[2] In this paper we attempt to determine the spatial scale of the oscillation associated with these spectral peaks, and present some of its four-dimensional characteristics. To do this, long time series (5–10 years) of station pressure and upper air data from several, primarily tropical, stations have been subjected to spectral and cross-spectral analyses. To complement and expand on the spectral evidence, daily analyses of sea-level pressure are also studied. These analyses provide complete spatial coverage of sea-level pressure over the entire tropical belt for an 18-month period during the IGY which is included in most of the station time series. Upper air data from several tropical stations during the IGY are also examined.

The results of the spectral analyses of the pressure records are presented first, showing locations which have a peak in the frequency range of interest ($\sim$1/40–1/50 day^{-1}) and those which do not. This provides a first approximation to the geographic boundaries which define the region where the pressure oscillation is an important feature. Spectral results from analysis of a limited amount of station pressure data available from the 1890's are then shown giving evidence that the oscillation has a degree of stationarity in time. The phase relationships and coherence-squared statistics based on cross spectra, which are discussed next, provide further clues concerning the nature of the pressure oscillation. The results from the spectral and cross-spectral analyses of the upper air data follow. The IGY pressure data is then examined to aid in the interpretation of the spectral results. The behavior of the upper level wind at a few stations during the IGY period is presented and, finally, a brief description of the phenomenon consistent with the aforementioned evidence is presented.

2. Data

The time series of station pressure was assembled from the rawinsonde records available at NCAR.[3] Most of these data were originally obtained from NOAA's National Climatic Center in Asheville, N. C. The station pressure, to the nearest whole millibar, from one sounding per day (usually at 0000 GMT) was included. If there was no available datum for a given day at the appropriate time, it was generated by a linear interpolation in time. Table 1 lists the stations,

[1] The National Center for Atmospheric Research is sponsored by The National Science Foundation.

[2] Referred to hereafter as MJ.

[3] For a description of data available at NCAR as of 5 May 1971 see UCAR GARP Council Information Bulletin No. 5.

TABLE 1. Stations used in pressure analysis.

Station	Time (GMT)	Latitude (deg, min)	Longitude (deg min)	Elevation (m)	Date series starts	No. of days in series	Interpolations (percent)	Mean station pressure (mb)	Remarks
Abidjan	06	5 15N	3 56W	7	1 Jun 57	2688	27.5	1010.7	1
Aden	00	12 49N	45 02E	3	1 Jul 57	2304	0.8	1008.1	
Ascension	00	7 58S	14 24W	79	1 Jul 58	1984	1.5	1005.4	
Balboa	00	8 59N	79 33W	69	16 Dec 59	2656	0.5	1001.4	2
Canton	00	2 46S	171 43W	4	1 Jul 57	3552	0.3	1008.8	
Campbell	00	52 33S	169 09E	19	1 Jul 57	3552	0.9	1002.6	
Curacao	00	12 11N	68 58W	8	1 Jul 57	2432	1.7	1009.4	
Dakar		14 44N	17 30W	24	1 Jul 57	2106	0.5	1008.3	3
Eniwetok	00	11 21N	162 21E	5	1 Jul 57	3168	2.0	1010.4	
Guam	12	13 33N	144 50E	111	1 Jul 57	3168	0.5	998.4	
Johnston	12	16 44N	169 31W	3	1 Jul 57	2862	2.8	1013.6	
Lihue	12	21 59N	159 21W	45	1 Jul 57	3168	0.3	1012.8	
Clark AB	00	15 11N	120 33E	143	28 Dec 57	3008	1.9	991.7	
Majuro	12	7 06N	171 24E	3	1 Jul 57	2816	5.0	1009.6	4,5
Midway	12	28 13N	177 23W	9	1 Jul 57	3168	11.0	1018.1	6
Nandi	00	17 45S	177 27E	18	1 Jul 57	3168	0.5	1007.7	
Raoul	00	29 15S	177 55W	49	1 Jul 57	3168	0.5	1012.1	
Recife	12	8 07S	34 55W	3	1 Jan 59	2192	7.2	1016.3	
San Juan	00	18 26N	66 00W	22	1 Jul 57	2736	0.4	1014.6	
Shemya	00	52 43N	174 06E	37	1 Jul 57	2048	3.8	1003.2	
Singapore	00	1 21N	103 54E	10	1 Jan 59	3008	1.2	1008.8	
Truk	12	7 27N	151 50E	2	1 Jul 57	2816	0.3	1009.3	5
Wake	12	19 17N	166 39E	0	1 Jul 57	3168	0.1	1014.1	
Yap	12	9 31N	138 08E	17	1 Jul 57	2816	2.3	1007.4	5
Gan	12	00 41S	73 09E	2	1 Jan 60	2624	0.2	1494 m	7

1. Data every other day to 1 Jul 61 and data at 0000 GMT from 1 Jun 64 through 9 Oct 64; no adjustments made for time differences.
2. Approximately 60 values taken from nearby Howard AFB records.
3. Data at 0600 GMT 1 Jul 57 to 19 Jan 60, 1200 GMT 20 Jan 60 to 31 May 60, 0000 GMT 1 Jun 60 to 30 Nov 61, 1200 GMT 1 Dec 61 to 6 Apr 63; no adjustments made for time differences.
4. Four consecutive months of data in middle of series interpolated.
5. Data at 0000 GMT 1 Jul 57 to 31 Aug 57, 1200 GMT 1 Sep 57 to 31 Aug 63, 0000 GMT 1 Sep 63 to series end; all data adjusted to 1200 GMT (see text).
6. Seven periods of approximately 20 consecutive values interpolated.
7. 850-mb heights used instead of station pressure.

station locations, Greenwich time of the observations that were used, beginning dates of the series, the number of days included in the series, the percentage of interpolations required, and the mean value of the series. Exceptions and special comments are noted by means of numbered remarks. Majuro, Truk and Yap Islands each had a considerable set of their data recorded at 1200 GMT and another, somewhat shorter set, recorded at 0000 GMT. Averages of the 0000 and 1200 data were computed separately. The difference between these averages was then included in the 0000 set to, in effect, adjust the entire record to 1200. In each case this difference was less than 0.5 mb.

A series from Nauru (0S, 161E) and one from Dar es Salaam (7S, 39E) were assembled from observations published by the former Deutsche Seewarte (1887–1922). The Nauru record consists of one pressure reading per day for 1476 days beginning on 1 January 1894. A sizable portion of the Nauru record was missing. Approximately 100 values were inserted from a record from Uyelang (10N, 161E), which were adjusted by taking into account the difference between their respective mean values. Thirty-four additional missing values were replaced by linear interpolations in time. The Dar es Salaam record consists of one pressure reading per day for 6080 days beginning on 1 December 1895. This record had 15 missing values which had to be replaced by interpolations in time.

The IGY data was in the form of sea-level pressure values at 5° intervals of latitude and longitude from 25S to 25N. These pressure values were digitized to the nearest whole millibar from IGY World Weather Maps, Part II, Tropical Zone (Deutscher Wetterdienst Seewetteramt, 1965). The digitized data were provided to us on cards by the Seewetteramt, Hamburg, Germany. These data were subsequently processed and made available on magnetic tape at NCAR.

Time series of wind and temperature were assembled for 14 tropospheric and stratospheric levels. In addition the time series of water-vapor mixing ratios were examined from the 1000-, 850-, 700-, 600- and 500-mb levels at most stations. As in the case of the pressure records, if there was no available datum for a given day at a given level, it was usually generated by a linear interpolation in time. Deviations from this method sometimes occurred if on a given day there were data available at other levels. Table 2 lists the stations, Greenwich time of the observations that were used, beginning dates, and number of days included in the upper air series. Necessary interpolations varied

TABLE 2. Stations used in upper air analysis.

Station	Time (GMT)	Date series starts	No. of days in series
Nairobi	0000	1 Jul 57	2000
Singapore	0000	1 Jan 60	2624
Truk[1]	1200	1 Jul 57	2862
Canton	0000	1 Jun 57	3584
Balboa	1200	1 Jul 57	1764
Ascension	0000	1 Jul 58	1984

[1] Data at 0000 GMT 1 Jul 57 to 31 Aug 57, 1200 GMT 1 Sep 57 to 31 Aug 63, 0000 GMT 1 Sep 63 to series end; no adjustments made for time differences.

between stations and levels. They were on the order of 2.5–5.0% in the lower troposphere and 5.0–7.5% in the upper troposphere. The percentage of required interpolations for stratospheric levels increased markedly. However, since the manifestation of the oscillation decreased rapidly in the stratosphere, the 100-mb level is the highest level at which the spectral results are discussed.

3. Results of spectral analyses of station pressure data

The method of estimating spectra, cross spectra, and band-pass filtered data is outlined in MJ. The results of the spectral analyses of the pressure data are presented in Fig. 1 for most of the stations studied. The bandwidth of each of the spectra varied somewhat, but all were very near 0.008 day^{-1}. Only those spectral estimates at frequency intervals of 0.005 day^{-1}, beginning at 0.000 day^{-1} and extending to 0.070 day^{-1}, are plotted. No significance limits are indicated in this figure. In MJ the statistical significance of the spectral peak in the 40–50 day period range for Canton was carefully established using *a posteriori* sampling theory. One would expect that similar statistically significant peaks would appear in the analyses of pressure records from nearby stations simply because of their proximity. Stations at locations far from Canton may or may not show spectral peaks near the period of interest. For those that do, it may be that the peak is associated with the same physical phenomenon occurring in the equatorial Pacific, but this association is best evaluated by the coherence statistic which is discussed in Section 5.

It is evident from the spectra presented that all stations within about 10° of the equator and the region westward from Curacao to Singapore, have marked peaks near the frequency range of interest. In MJ it was noted that spectra from Singapore and Balboa showed no clear indication of the oscillation. This conclusion was based on spectra computed for shorter records of wind data at only two levels. The spectra of their longer pressure records, not considered in MJ, do show peaks in the frequency range of interest. The stations available in the Atlantic region show little evidence that disturbances with a period of 40–50 days are any more important than those with 30- or 60-day periods.

The spectra presented in Fig. 1 indicate that the oscillation may affect an extremely large portion of the equatorial belt, extending at the least across the entire Pacific Ocean.

4. Evidence of time stationarity

The spectrum of the daily values of the station pressure recorded at 0700 LST for four years of record at Nauru is shown in Fig. 2. It is very similar to the spectrum of the pressure at Canton shown in Fig. 1. Since the Nauru data from the 1890's and the more

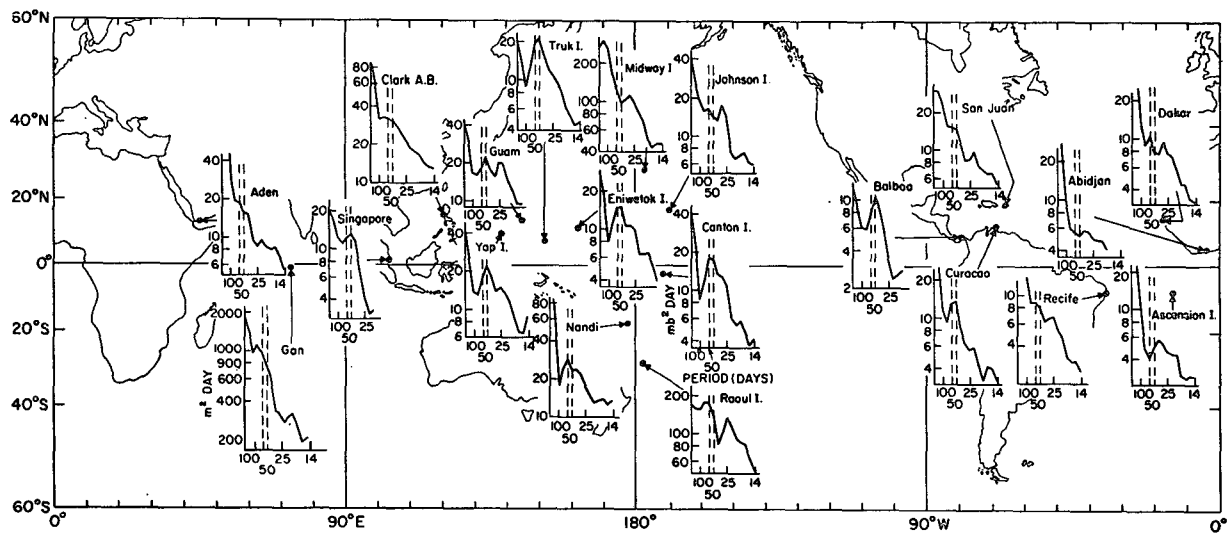

FIG. 1. Variance spectra for station pressures at several locations. Units for ordinates (mb^2 day) and abscissas (period in days) are indicated on spectrum for Canton Island. Ordinates are logarithmic and abscissas are linear with respect to frequency. The 40–50 day period range is indicated by the dashed vertical lines.

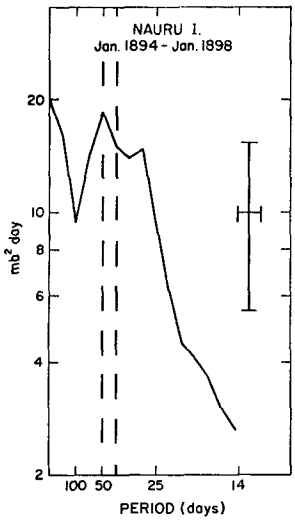

FIG. 2. Variance spectrum for station pressures at Nauru I. (0°24'S, 161°0'E). Ordinate is logarithmic and abscissa (frequency) is linear. The 40–50 day period range is indicated by the dashed vertical lines. Prior 95% confidence limits and the bandwidth of the analysis (0.008 day^{-1}) are indicated by the cross.

recent Canton data can be said to be statistically independent, it seems appropriate, in this case, to estimate the level of significance of the peak in the frequency range of interest. The 95% prior confidence limits are indicated, and even conservative estimates of the background spectrum suggest that this peak is significant at this level. We can, therefore, be reasonably confident in accepting the peak as a characteristic of longer records than those examined.

The spectrum of the very long record available from Dar es Salaam was computed for two segments of 2754 days each. The first segment begins on 1 December 1895 and consists of pressure values recorded at 1400 LST. The second segment consists of values recorded at 0700 LST and begins on 1 January 1905. In Fig. 3 the results of the spectrum analysis of each segment are plotted along with their average. Spectral estimates are plotted only at each 0.005 day^{-1} frequency interval in Figs. 2 and 3. The average spectrum has 40 degrees of freedom or twice that of the individual spectra. The 95% prior confidence limits are indicated for the average spectrum. The peak at a 50-day period is significant, though only marginally so, at the 95% level.

We conclude from these two spectra that the 40–50 day oscillation is not a temporary phenomenon in the equatorial Pacific occurring only in the late 1950's and the 1960's but one that has appeared at other times. The Dar es Salaam record indicates that the oscillation may be present in East Africa although its manifestation there is not as strong as it is in the equatorial Pacific.

Moreover, the oscillation apparently is not highly tuned to a specific frequency. For example, the Canton spectrum presented in this study based on data from July 1957 to March 1967 and that from MJ based on data from June 1957 to March 1967 reach their maxima near a 44-day period. The discussion of the time dependence of the oscillation, based on 47-day bandpass filtered data presented in MJ, mentioned that an apparent annual modulation was strong from July 1957 through the winter 1960–61 and weak and hardly noticeable after that. Further inspection of the filtered data reveals, in addition, that the mean amplitude of the oscillations, as evident in the 47-day band-pass filtered data, is smaller after the winter of 1960–61 than before. In order to determine how the apparent time dependence of the oscillation evident in the filtered data is reflected in the spectra, the Canton record was broken into two 1792 day sets. The first runs from 1 June 1957 through 27 April 1962. For the majority of this period the 47-day band-pass filtered data had relatively large amplitude. The second set begins on 28 April 1962 and runs through 24 March 1967, a period when the 47-day band-pass filtered data had relatively small amplitude. The spectrum of the first set has a very strong peak with a maximum near 46 days. The spectrum of the second set has a much weaker peak which has its maximum near 33 days. Similarly, the spectrum of the Balboa, C. Z., record reaches a peak near a 48-day period for the period from 1 July 1957 through 29 April 1962 and at a 33-day period for the period for 1 July 1962 through 14 June 1968. These results suggest that the phenomenon is one affecting a broader frequency band of the spectrum than originally thought. The "frequency range of interest" limited to 0.0245–0.0190 day^{-1} as defined in MJ may be too restrictive. We point out, however, that the apparent separation of peaks in the two

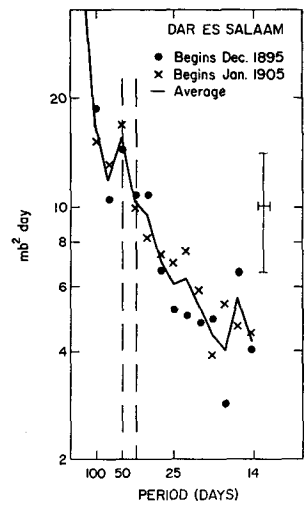

FIG. 3. Variance spectra for station pressures at Dar es Salaam (6°48'S, 39°18'E). Spectrum based on 2754-day series beginning 1 December 1895 indicated by dots. Spectrum based on 2754-day series beginning 1 January 1905 indicated by X's. Solid line is the average spectrum. The ordinate is logarithmic and abscissa (frequency) is linear. The 40–50 day period range is indicated by the dashed vertical lines. Prior 95% confidence limits for the average spectrum and the bandwidth of the analyses (0.005 day^{-1}) are indicated by the cross.

intervals is of the order of the bandwidth of the analysis. In discussion of the statistics we continue to refer to a frequency or period range of interest on the order of 40 to 50 days, but we recognize that this represents only approximate bounds on the period of the responsible physical phenomenon.

5. Results of the cross-spectrum analyses of station pressure data

It was speculated in MJ that the oscillation at Canton could be the manifestation of a large (thousands of kilometers) circulation cell oriented in a zonal plane near the equator. The evidence presented in Section 3 bears out the idea that the oscillation may be associated with something of very large, possibly of global, scale. In addition, the pressure oscillation appears to be confined to within about 10° of the equator. The estimation of cross spectra and coherence can serve as a further tool in establishing the areal extent of the phenomenon. Also, the phase relationships between locations will aid in determining whether or not the disturbance propagates zonally or simply behaves as a standing oscillation fixed in a zonal plane.

Canton Island was used as a reference station and its cross spectrum with all of the other 24 stations was computed. The coherence-squared, the background coherence-squared, and the phase angle that were estimated for the frequency band of interest are presented in Fig. 4. As a matter of convenience the coherence-squares and phase angles are averages over the particular bandwidth used (the average bandwidth was $\sim$0.008 cycle day^{-1}), with the low-frequency end set at 0.020 cpd. Therefore, they represent averages over the range of approximately 36–50 day periods. The background coherence was subjectively estimated by drawing a smooth line through the coherence values from low to high frequency and then this smoothed estimate was averaged over the same range. Now, we wish to estimate how confident one can be in assuming the various locations are being affected by the same phenomenon. Since nearby stations are usually highly coherent with Canton over much of the low-frequency range, we have chosen to indicate in Fig. 4 only those stations whose coherence-squares are significantly above the background continuum at the 95% level. By indicating coherence-squares which are above an arbitrary statistical significance level we are attempting to establish a relative base against which one can better estimate this confidence. Because so many locations have higher coherence-squares in the frequency range of interest, we can have a degree of confidence that they are being affected by the same phenomenon.

This confidence can be increased if the estimated phases behave in a reasonable manner. The phase angles are analyzed and a fairly consistent picture emerges over the entire Pacific and Indian Ocean region (Fig. 4). The analysis suggests that the disturbance occurs first at the stations in the western extreme of the region. It takes approximately 3 days for the disturbance to move from Singapore to Canton and another 3 days to reach Balboa. At the equator the disturbance propagates from west to east some 200° of longitude in 6–7 days. Evidence of such a rapid propagation suggests that the disturbance must in addition have some characteristics of a standing oscillation in order that it may be reflected by a period on the order of 45 days in a single station's time series. It propagates considerably slower in the meridional direction.

Since low coherence-squares are evident in the Atlantic-West African region it is possible that there is a source region for the disturbance somewhere over the Indian Ocean. The Dar es Salaam and Nauru records had only two contemporary years (1 December 1895–15 January 1898). In spite of the short data sample, their cross spectrum was computed. The background coherence-squared and the coherence-squared, determined in a manner similar to that

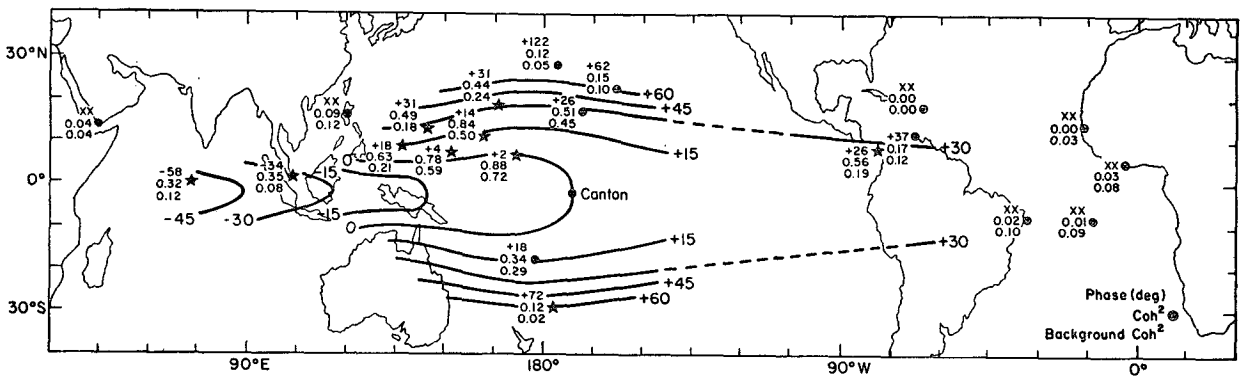

FIG. 4. Mean phase angles, coherence-squares, and background coherence-squares for approximately the 36–50 day period range of cross spectra between all stations and Canton. The plotting model is given in lower right-hand corner. Positive phase angles at a station means the Canton series leads that of the station. Stations indicated by a star have coherence-squares above the background at the 95% level. Mean coherence-squares at Shemya (52°43′N, 174°6′E) and Campbell I. (52°33′S, 169°9′E) (not shown) are 0.08 and 0.02, respectively. Both are below their average background coherence-squares.

discussed above, were about 0.25 and 0.45, respectively. With the 13 degrees of freedom available, this peak is significantly above the background at the prior 90% level. The phase angle indicates that Nauru trails Dar es Salaam by 58°, a result consistent with a disdisturbance originating over the Indian Ocean.

6. Results of spectral and cross-spectral analyses of tropospheric winds

The spectrum of the 150-mb zonal wind from Nairobi is presented in Fig. 5. A large spectral peak in the frequency range of interest is evident. A background spectrum was subjectively estimated and illustrated by the heavy line. The ratio between the total variance under the spectral curve in the period range of approximately 36–50 days and that under the background spectrum is indicated. This ratio was estimated for zonal wind spectra from all the stations and levels studied. These ratios are presented in Table 3, summarizing the many spectra. Ratios greater than unity indicate spectral peaks in the frequency range of interest. The spectra of station pressures from the Atlantic-West African region showed no indication that the pressure oscillation is present there. However, the zonal wind spectra at some levels from Ascension Island have relatively large peaks. It appears that in the upper troposphere, spectral peaks in the frequency range of interest occur at near-equatorial stations all the way around the globe.

It is interesting to estimate what percentage of the total variance is contained in the 36–50 day period range. For the 150-mb zonal wind at Nairobi (Fig. 5) it is about 10%. By way of comparison, we point out that the variance contained in the spectrum for periods <10 days is about 33% of the total variance.

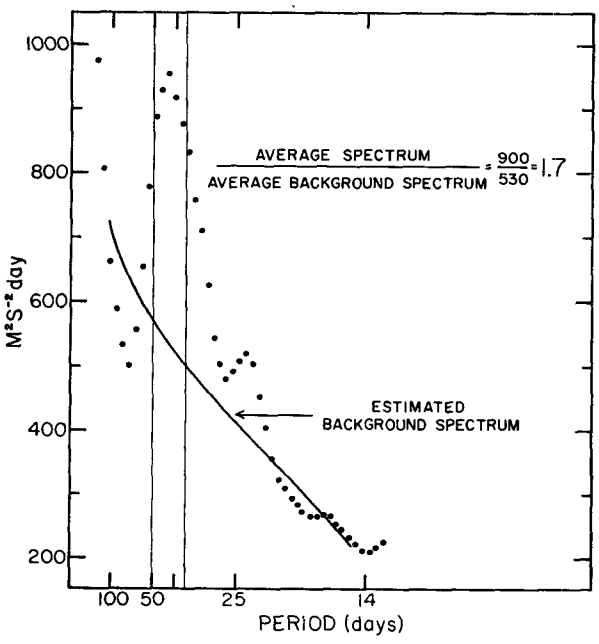

FIG. 5. Variance spectrum of the 150-mb zonal wind at Nairobi (1°19′S, 36°55′E, 1600 m elevation). Ordinate is linear and abscissa is linear with respect to frequency. See text for further explanation.

TABLE 3. Summary of zonal wind spectra.*

Station	Level (mb) 1000	850	700	600	500	400	300	200	150	100
Nairobi	X	X	1.0	1.0	1.0	0.8	1.0	1.2	1.7	1.9
Singapore	X	1.1	1.3	X	1.1	1.0	1.4	1.3	1.1	1.3
Truk	1.4	1.3	1.1	1.0	1.0	0.9	1.0	1.3	1.4	1.6
Canton	1.3	1.7	1.0	1.0	1.0	1.1	1.2	1.6	1.7	1.2
Balboa	1.0	1.0	1.0	1.1	1.4	1.2	1.3	1.2	1.4	1.2
Ascension	1.0	1.0	1.4	1.0	1.3	1.0	1.0	1.2	1.6	1.4

* Ratio of variance in frequency range of interest to estimated background variance. Ratios greater than 1 indicate spectral peaks. The X's indicate levels where no spectra were computed.

The Canton Island station pressure was again used as a reference station and its cross spectra with the zonal wind at all stations and levels were computed. The relevant results of these cross spectra are assembled in Table 4. Phase angles, coherence squares, and background coherence squares were determined as discussed in Section 5. Because many coherence squares are considerably above the background coherence squares one could, with some dgreee of confidence, assert that the oscillations in the Canton pressure record are somehow related to the corresponding oscillations in the zonal winds at the other stations. To learn something of this relationship we now consider the phase angles. If one assumes that the pressure oscillation at Canton is at its maximum, then, from the phase angles in Table 4, it is possible to determine the instantaneous character of the zonal wind oscillation at all levels and stations. This is done schematically in Fig. 6. The phase of the zonal wind oscillation at a given level and location is indicated by the length and direction of the plotted wind arrows. The unit length represents the maximum excursion at each location and is indicated in the lower left corner. From the phase angle, the local changes of zonal wind with time can also be determined, and their signs (+, −, 0) are indicated at the tail of the arrows. A fairly consistent picture emerges. Shown at the top of Fig. 6 is a model of the upper tropospheric (400–150 mb) zonal wind disturbance. It takes the form of an asymmetrical wave (i.e., the zonal wind goes from maximum westerly to maximum easterly in only 90° of longitude) extending all the way around the earth. This model is consistent with the plotted wind arrows and it will satisfy the local changes of zonal wind if, like the pressure disturbance, it has an eastward component of motion. At the bottom of the figure is a model for the lower tropospheric disturbance. It is similar to that for the upper trophosphere although it is out of phase and apparently confined to nearly the same region as that of the pressure disturbance. The wind arrows and local changes at 600 and 500 mb at Balboa do not fit with

TABLE 4. Summary of cross-spectral results between Canton pressure and zonal winds.*

	Level (mb)										
	1000	850	700	600	500	400	300	200	150	100	
Nairobi											
Phase (degree)			144	134	154	−85	−86	−86	−90	−107	d.o.f.=31
Coh²			0.20	0.27	0.17	0.11	0.22	0.39	0.51	0.33	95% limit=0.19
Background Coh²			0.09	0.10	0.07	0.09	0.08	0.18	0.23	0.15	
Singapore											
Phase (degree)		−150	−129		−101		−26		15	−89	d.o.f.=38
Coh²		0.24	0.43		0.48		0.12		0.31	0.17	95% limit=0.15
Background Coh²		0.22	0.12		0.20		0.09		0.16	0.09	
Truk											
Phase (degree)	−70	−68	−85	−98	−109	−126	149	129	123	93	d.o.f.=42
Coh²	0.32	0.50	0.50	0.48	0.29	0.18	0.18	0.27	0.26	0.18	95% limit=0.14
Background Coh²	0.10	0.19	0.17	0.09	0.08	0.02	0.05	0.07	0.08	0.09	
Canton											
Phase (degree)	−5	−9	−63		180	−75	180	172	158	164	d.o.f.=53
Coh²	0.34	0.41	0.11		0.14	0.25	0.28	0.36	0.38	0.19	95% limit=0.11
Background Coh²	0.08	0.08	0.06		0.09	0.07	0.09	0.13	0.19	0.13	
Balboa											
Phase (degree)				−44	−80	−120	−144	−165	−158	−144	d.o.f.=27
Coh²				0.23	0.21	0.44	0.53	0.60	0.58	0.20	95% limit=0.21
Background Coh²				0.06	0.11	0.33	0.30	0.31	0.31	0.11	
Ascension											
Phase (degree)						−83	−72	−100	−91	−87	d.o.f.=27
Coh²						0.22	0.33	0.47	0.57	0.32	95% limit=0.21
Background Coh²						0.05	0.05	0.08	0.13	0.17	

* Average phase (negative indicates Canton pressure trails), coherence square, and estimated background coherence square for the frequency range of interest. The X's indicate levels where no cross spectra were computed. Blanks are levels where coherence squares were less than their background coherence squares. The degrees of freedom for the respective series and the 95% significance level above an expected zero coherence are given for each station.

this low tropospheric model since, for an eastward propagating disturbance, they imply that maximum easterlies are to their west.

At Canton, there is no regular phase propagation with height from lower to upper troposphere, but only an abrupt phase shift occurring in the middle troposphere. At other locations there is some indication of vertical phase propagation, most notably between the 150- and 100-mb levels. It appears that at 100 mb, when the station pressure at Canton is a maximum, maximum

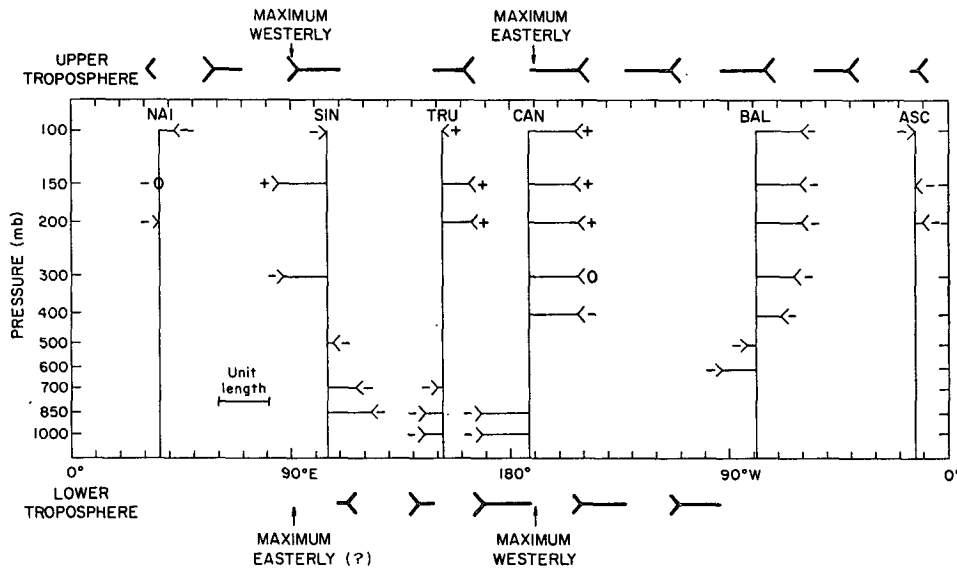

FIG. 6. Zonal wind oscillation in the equatorial plane at the time when the station pressure is a maximum at Canton based on the phase angles of Table 4. The unit length represents the maximum excursion at each location. The +, −, or 0 at the tail of each wind arrow represents the sign of the instantaneous local change of the zonal wind. Arrows are plotted only at levels whose coherence squares from Table 4 are above their background coherence square, and whose spectra, as tabulated in Table 3, indicate a peak. Heavy arrows at the top and bottom represent a schematic of the upper and lower tropospheric wind disturbance that is consistent with the plotted wind arrows and that will satisfy the local changes if it propagates eastward.

westerlies lie between Singapore and Truk. For an eastward propagating disturbance this represents an eastward slope with height or downward phase propagation with time. Nairobi, Singapore and Truk show this same vertical structure in the 150–100 mb layer while Canton, Balboa and Ascension indicate upward phase propagation with time.

Spectra of the meridional wind do not show the pronounced peaks in the frequency range of interest that those of the zonal wind show. Peaks that do occur are relatively small. Evidence presented in Section 9 indicates that mass flows in and out of the equatorial belt with the oscillation so that the meridional wind must be involved. However, the meridional motions required are very small and it is not surprising that the spectral analysis fails to clearly resolve them.

7. Results of spectral and cross-spectral analyses of tropospheric temperatures and water vapor mixing ratios

Spectra of temperatures were computed at the same levels as those of the tropospheric winds. In addition, water vapor mixing ratio spectra were computed at several low tropospheric levels.

We begin by discussing the temperature spectra at Truk, since they are very similar to those for Canton which were reported in MJ. Peaks are evident in the temperature spectra throughout the middle and upper troposphere, although they are not as pronounced as those typical of zonal wind spectra. Cross spectra were computed between Truk's temperature at each level and the Canton Island station pressure. In the lower troposphere there are relatively small peaks in the coherence squares in the frequency range of interest, and the phase angles are all within about 20° of 180°. At levels between 500 and 200 mb, coherence squares are very high (on the order of 0.60) and no phase angle differs by more than 5° from their mean of −159° (the negative sign indicates that temperature leads Canton pressure).

From this and from Table 2 in MJ, one can calculate that low station pressure at Canton and Truk (Fig. 4 shows that Truk's station pressure trails that at Canton by only 4°) are accompanied by correspondingly high tropospheric temperatures. At 150 mb the coherence square in the frequency range of interest is only slightly above the background coherence squares and the phase is −156°. The coherence square for the 100-mb temperature is again high (0.55) but the phase angle shifts abruptly to a positive 25°. There is a similar phase shift between 150 and 100 mb at Canton, indicating that at these two stations low station pressure is accompanied by low temperatures at 100 mb, a fact not inconsistent with the rapid weakening of the zonal wind disturbance in the lower stratosphere there. The hydrostatic equation was used to link pressure, temperature and geopotential height variations in a quantitative manner in MJ.

TABLE 5. Summary of cross-spectral results between Canton pressure and 100-mb temperatures.*

	Coh²	Background Coh²	Phase (deg)
Nairobi	0.20	0.07	165
Truk	0.55	0.06	25
Canton	0.20	0.15	45

* Average phase (negative indicates Canton pressure trails), coherence squares, and estimated background coherence square for frequency range of interest.

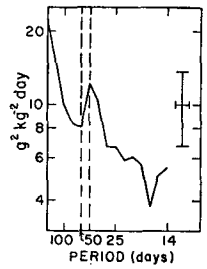

FIG. 7. Variance spectrum of the 700-mb water-vapor mixing ratio spectra for Truk. Ordinate is logarithmic and the abscissas are linear with respect to frequency. The 40–50 day period range is indicated by the dashed vertical lines. Prior 95% confidence limits and the bandwidth of the analyses (0.008 day^{-1}) are indicated by the cross.

Similar spectra of tropospheric temperatures at Balboa, Ascension, Nairobi and Singapore occasionally show small peaks and some degree of coherence with Canton station pressure; however, these features are spotty and we could glean no consistent picture from them. However, one interesting phenomenon, and one that is no doubt intimately related to the oscillation, is the presence of large peaks in the temperature spectra in the frequency range of interest at 100 mb that are evident at Nairobi, Singapore, Truk and Canton. In addition, there is a degree of coherence between Canton station pressure and the 100-mb temperatures at Nairobi, Truk (as we have just seen) and Canton. The resulting phase angles presented in Table 5 suggest that the 100-mb temperature disturbance also has a degree of eastward propagation.

The spectrum of the 700-mb water vapor mixing ratio at Truk is presented in Fig. 7. A sharp spectral peak is evident whose maximum is near the high-frequency portion of the frequency range of interest. Some of the mixing ratio spectra from other locations show small peaks in the period range of interest; however, none are as well marked as this one at Truk.

In an attempt to learn if mixing ratio variations were a part of the oscillation, we again computed cross spectra using the Canton station pressure as a reference series. The results of these cross spectra for 700-mb mixing ratios are summarized in Table 6. At Singapore, Truk and Balboa, coherence squares tend to peak near the frequency range of interest. From the phase angles presented in Table 6 and Fig. 4, one can estimate

TABLE 6. Summary of cross spectral results between Canton pressure and 700-mb mixing ratio.*

	Coh²	Background Coh²	Phase (deg)
Nairobi	0.01	0.03	
Singapore	0.23	0.03	105
Truk	0.27	0.03	−128
Canton	0.00	0.00	
Balboa	0.21	0.09	−72
Ascension	0.04	0.07	

* Average phase (negative indicates Canton pressure trails), coherence squares, and estimated background coherence squares for frequency range of interest (at Balboa the average is centered on 0.019 day^{-1} where the coherence square peaks). Phase angles are included only if coherence squares are above estimated background coherence squares.

that low station pressures tend to be accompanied by high mixing ratios at Singapore and Truk, while at Balboa (because mixing ratio leads station pressure by about 90°) they are accompanied by mixing ratios going through their relative zero and increasing. Direct cross-spectral analysis between a station pressure series and its own mixing ratio series confirms these relations. Fig. 8, discussed in the next section, illustrates that the phase angles presented in Table 6 are also consistent with eastward propagation of maximum (and minimum) 700-mb mixing ratios.

8. Summary of spectral and cross spectral results

In Section 3 we have seen that station pressure spectra have peaks in the 40–50 day period range at stations near the equator from at least Curacao westward to Singapore. Evidence that the oscillation has a degree of time stationary in the equatorial Pacific is discussed in Section 4. It was also noted that the "frequency range of interest" defined in MJ may be too restrictive since the frequency of the oscillation appears to change with time between somewhat larger limits. In Section 5 cross-spectral analysis indicated that the pressure disturbance moved rapidly eastward across the Pacific. This rapid propagation taken together with the relatively low frequency of the spectral peak suggests that the spatial structure of the pressure disturbance must vary with time while propagating eastward.

Spectral and cross-spectral studies of the zonal winds at several near-equatorial stations, as summarized in Fig. 6, show that the low tropospheric disturbance, which is manifested by both spectral peaks and a degree of coherence, is confined to the Pacific region, while that of the upper troposphere affects the entire circumference of the globe. Phase angles indicate that the upper tropospheric disturbance has a predominantly eastward component of motion, and that it is approximately out of phase with the lower tropospheric disturbance over the Pacific. Evidence concerning the role of the meridional wind is scanty and no conclusions can be drawn at this time.

From the spectrum analyses of tropospheric temperatures we conclude that in the Central Pacific low station pressures are accompanied by high temperatures through most of the troposphere. This nearly out-of-phase relationship changes to a nearly in-phase relationship at 100-mb. The 100-mb temperature spectrum shows relatively large peaks in the frequency range of interest at several stations. Cross spectra with the station pressure at Canton indicate that the 100-mb temperature disturbance also propagates eastward. Cross spectra between Canton pressure and low tropospheric water-vapor mixing ratios provide evidence that, in the Pacific, mixing ratios vary with the oscillation. High mixing ratios tend to accompany low station pressures at Singapore and Truk.

Fig. 8 is presented to summarize the spectral results. The phase angles plotted are those from the cross spectra between Canton station pressure and the specific variable. They have been taken from Fig. 4 (station pressure), Table 4 (150- and 850-mb zonal wind), Table 5 (100-mb temperature), Table 6 (700-mb mixing ratio), and also results from the 300-mb temperature cross spectra. One can approximate the phase angle between any two variables at a given station from the vertical distance between them in Fig. 8. All the points plotted in Fig. 8 relate to variables that show spectral peaks in the frequency range of interest (excepting 700-mb mixing ratios at Singapore and Balboa), and are coherent with the Canton pressure at a high level of statistical significance (at least significantly above an expected zero coherence at the 95% level). Ultimately we wish to describe the physical phenomenon responsible for these spectral results. Because this is so, any statistical criterion that we use to establish if and how a variable is related to the

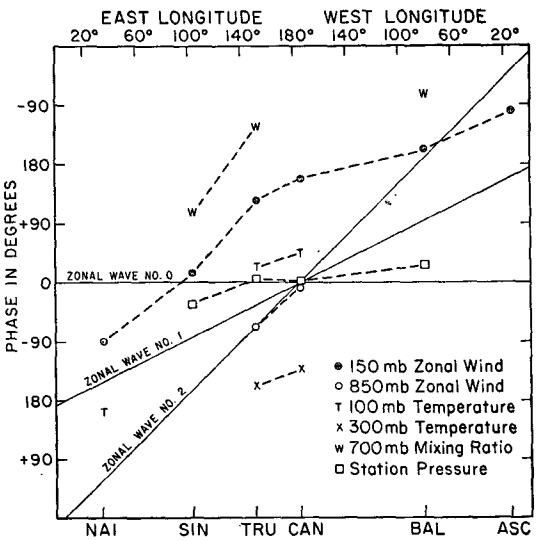

FIG. 8. Phase angle between given variables at given stations and the station pressure at Canton Island as given by the cross-spectral analyses. See text for further explanation.

oscillation is necessarily an arbitrary one. Fig. 8 does not, therefore, necessarily represent the *only* variables associated with the oscillation. However, it does portray variables and their relationship to the Canton pressure record that one can be reasonably sure, based on the spectral evidence, *are* associated with the oscillation. For comparison, lines indicating the locus of phase angles expected for eastward propagating zonal wavenumbers 1 and 2 pressure disturbances are included. The zonal wavenumber zero line represents an oscillation in the zonal mean pressure. A standing zonal wavenumber 1 disturbance would have one region, 180° in longitudinal extent, exactly in phase and a second region exactly out of phase separated by the two nodal points of the wave.

9. Large-scale pressure changes during the IGY period

To this point, only evidence based on spectral analyses has been presented. We now attempt to look at the oscillation in a synoptic sense. First, that portion of the Canton station pressure record which was concurrent with available IGY data (July 1957–December 1958) was examined to determine dates of maximum and minimum pressure. In Fig. 9 the actual Canton station pressures from 1 October 1957 through 31 May 1958 are plotted along with the same pressures after they have been subjected to a 45-day band-pass filter. Fairly strong oscillations are evident in the filtered data with peak-to-trough amplitudes from 1.5–2.0 mb. These oscillations are reasonably well defined in the plot of the actual (unfiltered) data as well. Dates of maximum or minimum pressure at Canton were selected with the aid of a plot similar to that presented in Fig. 9, but extending over the entire 18-month period of July 1957 through December 1958. Horizontal pressure analyses were then made for 5-day averaged values taken from the daily IGY maps. The 5-day averages were centered on dates corresponding to these relative maxima or minima. Five-day averaging was used to minimize the effects of the 5-day pressure waves evident in the tropics (Wallace and Chang, 1969; Misra, 1971[4]). Four of these analyses for the Pacific region are shown in Fig. 10. The 5-day averaged pressure maps for the "high pressure" dates (20 October 1957 and 4 December 1957) have pressure values less than 1010 mb but greater than 1008 mb over most of the equatorial area. Those for the "low pressure" dates (12 November 1957 and 26 December 1957) have pressure values less than 1008 mb, and some less than 1006 mb, over most of the equatorial region.

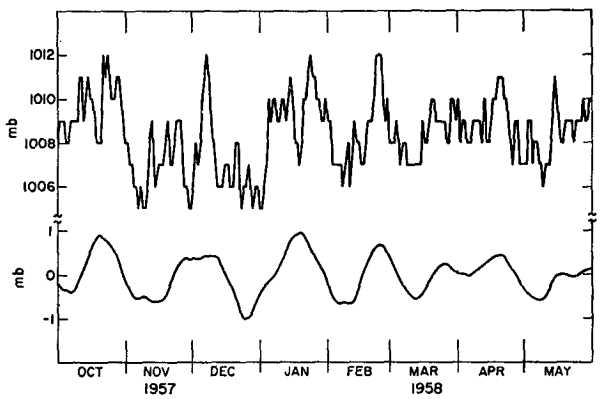

FIG. 9. Actual station pressures at Canton (top) and the corresponding pressures treated with a 45-day band-pass filter (bottom).

If many similar pressure maps are computed, based on dates determined from the manifestation of the oscillation in the Canton time series, and these maps averaged, one can construct mean pressure maps for times of high or low pressure at Canton. Further, in addition to the mean pressures at dates of Canton's maximum and minimum, one can compute mean pressures over all longitudes at several other dates selected by virtue of their positions relative to the oscillation as revealed in the Canton time series. A mean disturbance can be constructed in a manner analogous to the compositing techniques used successfully by many authors in studies of tropical circulations. To illustrate, consider that the wave form in the time series of Canton pressures is a series of simple waves with arbitrary peak-to-trough amplitude. One such wave is depicted in Fig. 11. Pressures are then determined for all longitudes at the dates indicated (in Fig. 11) by A, B, C, etc. By examining the mean pressure at each longitude at all those dates corresponding to A, B, C, etc., in successive order we can construct a picture of a mean disturbance in both space and time. During the July 1957–December 1958 period all dates of maximum and minimum pressure were determined from the 45-day band-pass filtered data. Eleven complete oscillations could be examined. The time interval between successive maxima and minima varied somewhat. The median time interval was 23 days and there were only three occasions when it fell outside of the 18–25 day range. Intervals between the time of maximum and minimum pressure were simply divided by three to determine intermediate dates. Consequently, the average interval between times represented by successive letters is 5–6 days.

The resulting mean pressure disturbance along the equator is presented in Fig. 12. From approximately 70W eastward to 40E the mean pressures do not vary in a consistent fashion, while over the entire Indian and Pacific Ocean region an eastward propagating disturbance is evident. The very small deviations between about 70W and 40E are expected when one considers the spectra results shown in Fig. 1 and the coherence squares in Fig. 4. The eastward propagation

[4] Misra, B. M., 1971: A time-series analysis of global atmospheric pressure. *Preprints of Papers Intern. Symp. on Probability and Statistics*, Amer. Meteor. Soc., 1–4 June 1971, Honolulu, Hawaii, 41–46.

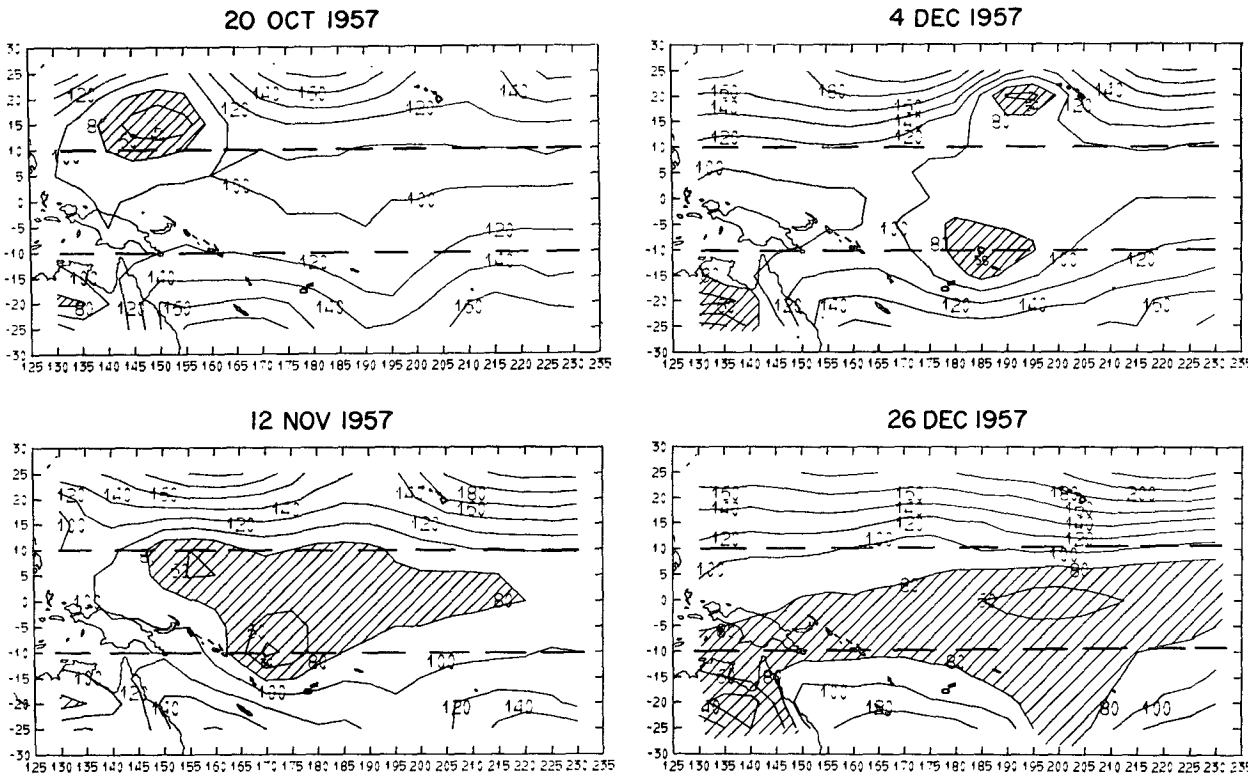

FIG. 10. Analyses of 5-day-averaged sea-level pressures over the Pacific during the IGY. Averages are centered on the date indicated above each chart. Contours are tenths of a millibar above 1000 mb. Hatched areas indicate pressures below 1008 mb. Degrees east longitude are indicated. Horizontal dashed lines represent 10S and 10N.

across the equatorial Pacific evident in Fig. 12 also corroborates the conclusion drawn from the cross-spectral evidence concerning eastward propagation there. It appears that the oscillation affects the Indian Ocean region and moves eastward out of it. The fact that anomalies do not always add to zero along the equator indicates that mass flows in and out of the equatorial belt with the oscillation.

10. Large-scale changes in the zonal wind during the IGY

A mean disturbance in the zonal wind at selected stations during the IGY was computed in a manner identical to that used to determine the mean pressure disturbance. The resulting 150 and 850-mb mean zonal wind disturbance is presented in Fig. 13. The out-of-phase relationship in mean zonal wind disturbances between upper and lower troposphere is clear, especially at Singapore, Truk, Canton and Christmas. Next, considering only the upper tropospheric disturbance, one sees that when pressures are rising in the Central Pacific (E–A), upper tropospheric winds there are becoming more easterly; at Singapore they are becoming more westerly, and only a small change is noted at Nairobi. These results are consistent with the cross-spectral evidence. Eastward movement of the upper tropospheric disturbance can best be seen by following the point dividing westerlies and easterlies. At time G this point is located between Nairobi and Singapore and it separates relatively large westerly and easterly flows. At time H it is east of Singapore; at time B it is east of Truk and separates somewhat weaker flows. We also note that the relatively large discrepancies between these observed winds and those that one would expect from a simple, eastward moving, zonal wavenumber 1 disturbance are consistent with asymmetric model presented in Fig. 6.

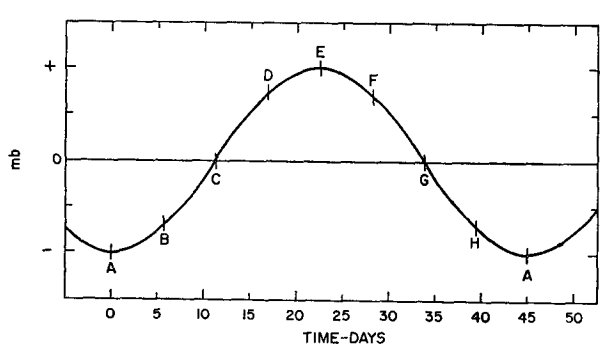

FIG. 11. Idealized depiction of simple pressure wave in the Canton time series. The ordinate scale is arbitrary although the average peak-to-trough amplitude during the IGY was 2 mb. The average period of 45 days is indicated on the abscissa.

The low tropospheric oscillation is evident at Singapore, Truk and Canton as is expected from the spectral results. In addition, there is evidence that the oscillation is reflected in the low tropospheric wind at Nairobi. Regions where there is large-scale convergence (divergence) in the 850-mb zonal wind are usually accompanied by regions of large-scale divergence (convergence) in the 150-mb zonal wind.

The temporal behavior of the disturbance at a given station can be extracted from the spatial behavior of the mean disturbance which is presented at given times in Fig. 13. This is done for the 150-mb zonal wind and for the sea-level pressures at the longitude nearest the given station from Fig. 12, and presented in Fig. 14. At Canton the wind and pressure disturbances are symmetric with maxima and minima 180° apart. At Singapore the disturbances are highly asymmetric with maxima and minima separated by only 90°.

Since only eleven waves are involved in these means there is likely to be some unrepresentativeness due to sampling fluctuations. In an effort to ascertain to what degree these mean disturbances are representative of the disturbances responsible for the spectral results, phase angles were computed based on the mean disturbance and compared with those for the 150-mb zonal wind of Table 4. This was done by first computing a covariance between the mean station pressure disturbance at Canton and the mean 150-mb zonal winds of Fig. 14. The mean Canton pressure disturbance was then lagged by 90° and a lagged covariance was computed. The covariance and lagged covariance are analogous to cospectral and quadrature spectral estimates. Their ratio gives an estimate of the mean phase angle. The resulting phase angles are within 15° of those of Table 4 for Nairobi, Singapore, Canton and Balboa, and within 30° for Truk. This relatively close correspondence leads us to conclude that temporal behavior of the disturbance as indicated by the mean picture presented in Fig. 14 is a representative one.

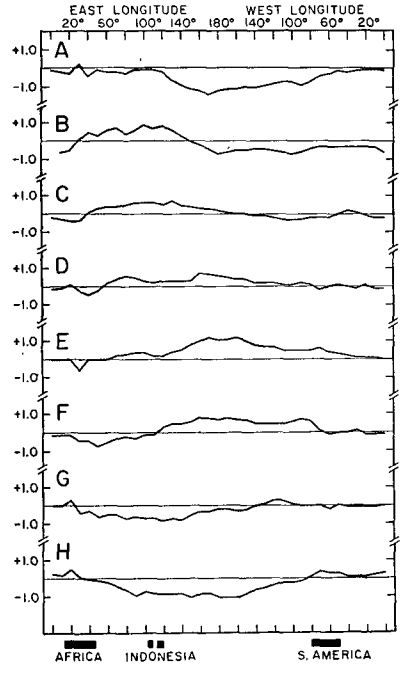

FIG. 12. Mean pressure disturbance along the equator for dates indicated symbolically by the letters at the left of each chart. The letters represent those dates whose relative positions with respect to the pressure oscillation in the Canton time series are indicated in Fig. 11. Each mean is the average of eleven individual 5-day averages which are centered on the appropriate date. The interval between the times represented by successive letters averages to 5–6 days. Data plotted at each 10° of longitude are anomalies from the 18-month average for the respective longitude.

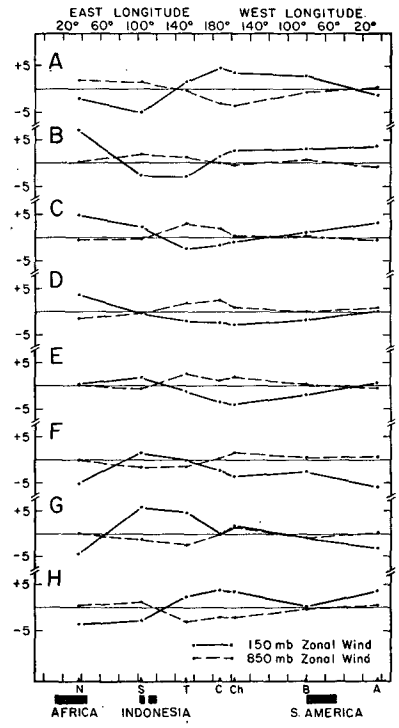

FIG. 13. Mean zonal wind disturbance at 850 and 150 mb for dates indicated symbolically by the letters at the left of each chart. The dates and averaging technique are identical to those of Fig. 12. Ordinate values are in m sec^{-1}. Data plotted for each station (N—Nairobi; S—Singapore; T—Truk; C—Canton; Ch—Christmas 2N, 157W; B—Balboa; A—Abidjan) are the anomalies from the 18-month average at that station.

The relationship between the 150-mb zonal wind and the local pressure at Nairobi is distinctly different from that at Truk, Canton and Balboa. They are in phase at Nairobi and out of phase at the other three stations. Another interesting feature is the rapid change from maximum westerlies to maximum easterlies at Singapore. Any physical phenomenon proposed to be responsible for the 150-mb zonal wind oscillation must, in addition, be consistent with these features.

11. Large-scale changes in tropospheric temperatures and water vapor mixing ratios during the IGY

The mean temperature disturbance, determined in an identical manner as that used in constructing the mean

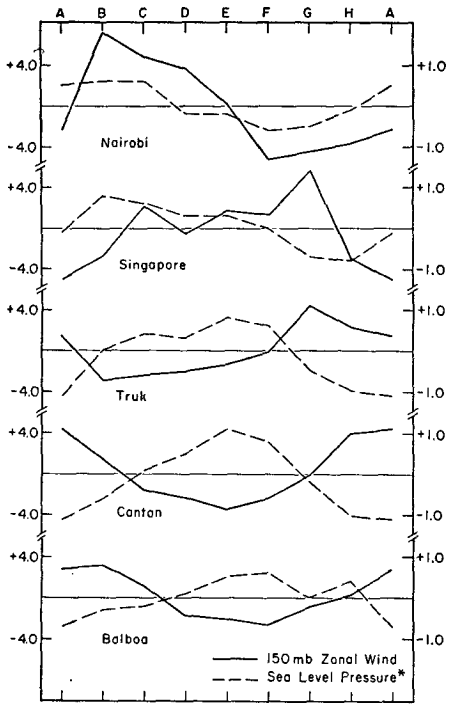

FIG. 14. Temporal behavior of the mean 150-mb zonal wind disturbance for several stations. Ordinate values on the left are m sec^{-1}. Times are indicated symbolically across the top of figure. Data are taken from Fig. 13. Also included is the temporal behavior of the mean sea-level pressure disturbance at the longitude nearest the given station. Ordinate values on the right are mb. This data is taken from Fig. 12, except for Nairobi (*) where a mean disturbance in station pressure is plotted because of the high altitude of that station.

pressure and zonal wind disturbances, indicates that a relatively warm troposphere at Truk, Canton and Christmas accompanies relatively low station pressure at Canton. This is expected from the spectral evidence. The mean amplitude of temperature changes is small, suggesting a peak-to-trough value of approximately 1.0K. The mean temperature oscillation at 300 and 100 mb at several stations is presented in Fig. 15. The 100-mb temperature is seen to be nearly out of phase with the 300-mb temperature. In addition, its peak-to-trough amplitude is approximately twice that at 300 mb at all stations except Balboa.

The 700-mb mixing ratio for the mean wave is also plotted in Fig. 15. The peak-to-trough amplitude at Singapore and Truk is 1 gm kg^{-1} and about 0.5 gm kg^{-1} at Balboa. These are the three stations at which mixing ratios showed a degree of coherence with the Canton pressure record. At all three the mean mixing ratio is in phase with the 300-mb temperature. Wallace (1971) has shown that there is a similar in-phase relationship between vertically averaged relative humidity and the 300-mb temperature in the 5-day synoptic-scale disturbances prevalent in the western Pacific. He also shows that these two variables are in phase with increased satellite brightness, indicating that high relative humidities and warm 300-mb temperatures are accompanied by enhanced convection. In like manner, it may be possible that increased mixing ratios in the 40–50 day oscillation are a sign of enhanced large-scale convection, which in turn is responsible for warmer tropospheric temperatures through locally realized latent heat release.

12. Discussion

It is clear that the 40–50 day oscillation evident in the Canton station pressure and upper air record is associated with a phenomenon of global scale. Spectra computed at many different locations indicate this large scale of the disturbance, while those computed at two different time periods show it has a degree of stationarity. The cross spectra indicate something of its spatial structure. The characteristics of the mean oscillation, determined from synoptic analyses, aid considerably in the interpretation of these cross-spectral results.

To summarize, we have presented in Fig. 16 a schematic depiction of time and space variations of the disturbance which are consistent with the amassed evidence. The pressure anomalies are taken from Fig. 12, the indicated zonal circulation cells are based on Fig. 13, and the tropopause anomalies are based on the 100-mb temperature of Fig. 15, assuming that relatively high

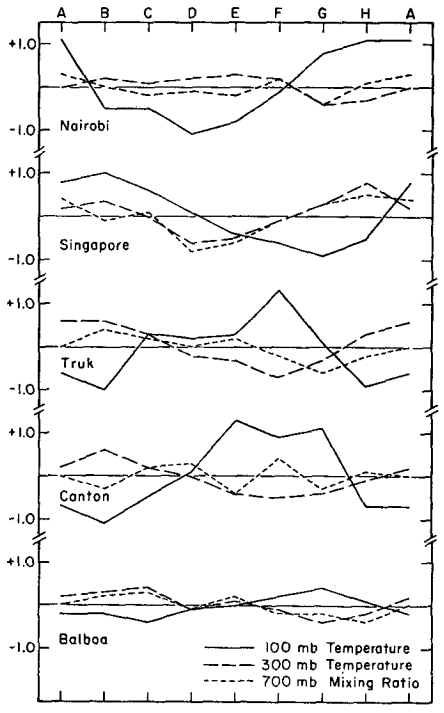

FIG. 15. Temporal behavior of the mean 300- and 100-mb temperature disturbances and the mean 700-mb mixing ratio disturbance at several stations. Ordinate values represent both °K and gm kg^{-1}. Times are indicated symbolically across the top of the figure. These mean disturbances were determined in a manner identical to that used for the data presented in Figs. 12–14.

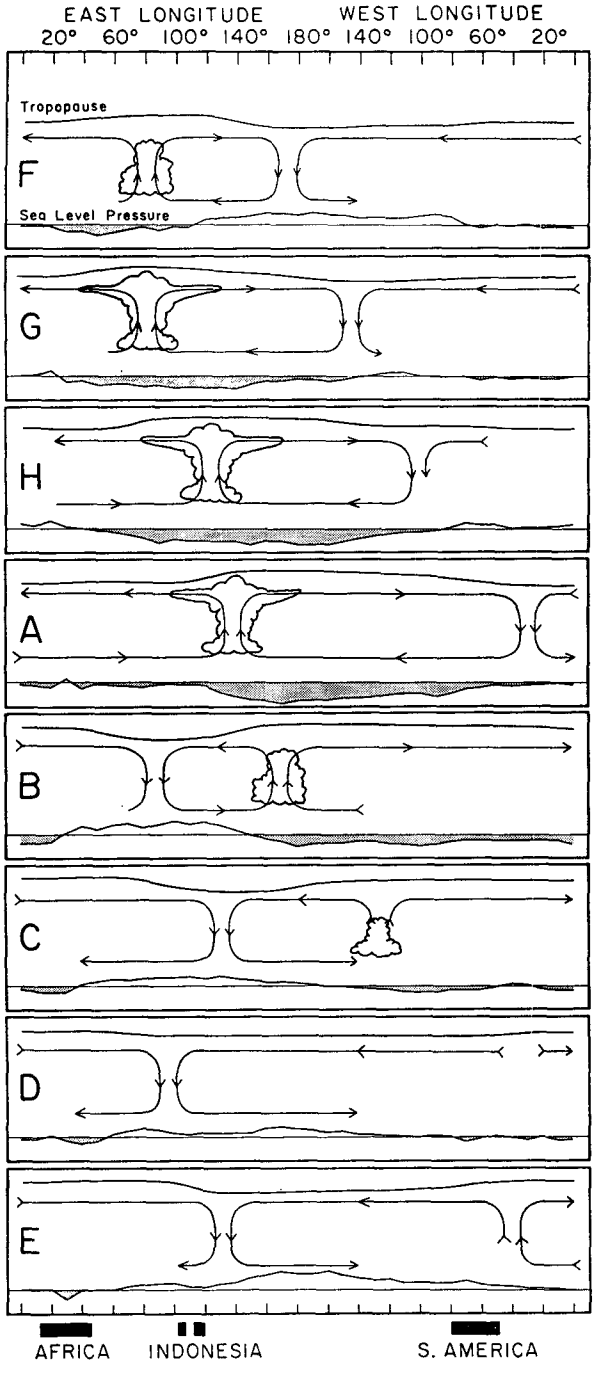

FIG. 16. Schematic depiction of the time and space (zonal plane) variations of the disturbance associated with the 40–50 day oscillation. Dates are indicated symbolically by the letters at the left of each chart and correspond to dates associated with the oscillation in Canton's station pressure indicated in Fig. 11. The mean pressure disturbance taken from Fig. 12 is plotted at the bottom of each chart with negative anomalies shaded. The circulation cells are based on the mean zonal wind disturbance presented in Fig. 13. Regions of enhanced large-scale convection are indicated schematically by the cumulus and cumulonimbus clouds. The relative tropopause height is indicated at the top of each chart.

100-mb temperatures correspond to relatively low tropopause heights.

While the enhanced large-scale convection indicated in Fig. 16 is somewhat speculative, the circumstantial evidence supporting it is considerable. It is indicated by the low tropospheric convergence and upper divergence of the zonal circulation cells, and by the evidence presented concerning the oscillation in mixing ratios and tropospheric temperatures. Moreover, both the horizontal scale and the large movements of mass associated with the oscillation require a considerable amount of energy. Ramage (1968) has emphasized the importance of the maritime continent (Indonesia and the Carolines) as a convective energy source. In addition, Bjerknes (1969) has described a west–east oscillation of the point of lowest pressure at the equator in this region. This oscillation has a time scale of two to four years with the point of low pressure varying from Western New Guinea (130E) to Canton Island (170W). The result is a movement of the "Walker circulation" which consists of a zonal circulation cell over the Indian Ocean and one over the Pacific Ocean (Bjerknes, 1970). In the low troposphere these circulations converge at the point of low pressure and rise in a large-scale updraft, while in the upper troposphere winds diverge from the updraft. This updraft is presumably accompanied by enhanced large-scale convection. Indeed, Krueger and Gray (1969) have suggested that observed heavy rainfall and extensive cloudiness located over Indonesia, New Guinea and northern Australia, and the corresponding low amounts of rainfall and cloudiness east of the dateline are associated with the Pacific branch of the Walker circulation. The time scale of this oscillation differs by more than an order of magnitude from that discussed here. However, the structure of the Walker circulation cells are similar to the structure proposed in Fig. 6, with the exception of the relationship of pressure and low-level zonal wind at Canton pointed out in MJ.

The behavior of the disturbance as indicated in Fig. 16 is as follows. There is a negative pressure anomaly over East Africa and the Indian Ocean at time F. We speculate that this is a time of increasing, large-scale convection over the Indian Ocean region. The zonal circulation cell to the east of the convection reaches only to the date line. Nairobi is under the influence of the western circulation cell and thus it experiences strong upper tropospheric easterlies and low surface pressures. This is consistent with the in-phase relationship there, pointed out in Section 10. By time G the pressure anomaly has spread eastward along with the eastern circulation cell. At time H the zonal circulation cells indicate that the center of large-scale convection has moved eastward across Indonesia. This accounts for the rapid shift from maximum westerlies to maximum easterlies at 150 mb between time G and A at Singapore. By time A the two circulation cells are nearly symmetric. At B the western cell

shrinks and pressures rise over the Indian Ocean signaling, we think, the weakening of the convection which is now centered near the dateline. Weak convection is still indicated at time C, primarily because the spectral evidence and that from the IGY period suggest that there is a weak maximum in the 700-mb mixing ratio at that time at Balboa. By time D there is no law tropospheric convergence accompanying the upper tropospheric divergence which is now located over the Atlantic. Because of this and the evidence that the oscillation does not affect pressures or low tropospheric winds in the Atlantic-West African region, a region of enhanced convection is not indicated at this time. The schematic at time E of Fig. 15, based primarily on the mean disturbance computed for the IGY, can be compared directly to that of Fig. 6, which was based solely on spectral evidence. Two nearly symmetric circulation cells result from the mean disturbance while the spectra suggested two asymmetric circulation cells. This apparent discrepancy is resolved when one considers that the phase angles based on the cross spectra are integrated for the entire wave form and thus reflect any asymmetries that occur.

Aside from a complete description of the physical phenomenon associated with the oscillation there is the question of its periodicity. Why does this oscillation have a preferred time scale? It could be associated with tidal effects in some sort of a beat fashion as discussed by Brier (1966). The fact that the oscillation does not appear to be highly tuned to a specific frequency speaks against this possibility. It is more likely that it is associated with some sort of a feedback mechanism as that of sea-surface temperatures and atmospheric circulation (Bjerknes, 1969; Krueger and Gray, 1969) or evaporation and precipitation (Kraus, 1959). The behavior of the 100-mb temperature suggests that there may be an eastward propagating wave in the tropopause height associated with the disturbance. Holton (1972) has shown that large-scale latent heat releases confined to a region of narrow longitudinal extent could generate the global-scale propagating waves that have been observed in the equatorial stratosphere. It is conceivable that in a similar fashion convection in the Indian and western Pacific Oceans generates the tropopause wave which travels around the earth (while the convection is weakening over the Central Pacific) in time to interact in some way to initiate convection again over the Indian Ocean. The propagation speed of the wave on the tropopause would then determine the time scale of the oscillation.

In conclusion we have shown that the 40–50 day oscillation evident at Canton is associated with a disturbance which affects the entire tropics. Though spectrum analyses indicate that the pressure oscillation is not an important feature in mid-latitudes of the Pacific Ocean, we feel that a tropical disturbance of this scale must affect other regions. Indeed, since the pressure anomalies presented in Fig. 12 often do not add to zero in the zonal plane there must be an interaction with other latitudes. The study presented here is being extended to determine how the 40–50 day oscillation in the tropics interacts with the weather of the extratropics. Other areas are being investigated to test the speculative model of the disturbance presented here. Satellite data can be used to confirm if, and to learn exactly how, convection is associated with the disturbance. Possible causes for the time scale of the oscillation are being studied. It is hoped that these current investigations will establish what role the 40–50 day tropical oscillation plays in the general circulation of the atmosphere, and for what reason it manifests this particular time scale.

Acknowledgments. We thank R. Jenne, D. Bundy, A. Cowley of NCAR, and W. Rudloff of the Seewetteramt, Hamburg, Germany, for their help in assembly and initial processing of the data. We further acknowledge the help of student assistants S. Endorf, C. Leary, C. Parsons and L. Sapp. R. Coleman drafted most of the figures and E. Workman typed the manuscript.

REFERENCES

Bjerknes, J., 1969: Atmospheric teleconnections from the equatorial Pacific. *Mon. Wea. Rev.*, **97**, 163–172.

——, 1970: Atmospheric interaction resulting from variable heat transfer at the equator. Studies in Climate Dynamics for Environmental Security, RM-6353-ARPA, The Rand Corporation, Santa Monica, Calif.

Brier, G. W., 1966: Evidence for a longer period tidal oscillation in the tropical atmosphere. *Quart. J. Roy. Meteor. Soc.*, **92**, 284–289.

Deutsche Seewarte, 1887–1922: Deutsche Überseersche Meteorologische Beobachtungen, I–XXIII.

Deutsche Wetterdienst Seewetteramt, 1965: International Geophysical Year (1957–58) world weather maps. Part II: Tropical zone 25°N to 25°S. Daily sea level and 500 mb charts. Einzelveröffentlichungen, Hamburg.

Holton, J. R., 1972: Waves in the equatorial stratosphere generated by tropospheric heat sources. *J. Atmos. Sci.*, **29**, 368–375.

Kraus, E. B., 1959: The evaporation precipitation cycle of the trades. *Tellus*, **11**, 147–158.

Krueger, A. F., and T. I. Gray, 1969: Long term variations in equatorial circulation and rainfall. *Mon. Wea. Rev.*, **97**, 700–711.

Madden, R. A., and P. R. Julian, 1971: Detection of a 40–50 day oscillation in the zonal wind in the tropical Pacific. *J. Atmos. Sci.*, **28**, 702–708.

Ramage, C. S., 1968: Role of a tropical "Maritime Continent" in the atmospheric circulation. *Mon. Wea. Rev.*, **96**, 365–370.

Wallace, J. M., 1971: Spectral studies of tropospheric wave disturbances in the tropical Western Pacific. *Rev. Geophys.*, **9**, 557–612.

——, and C.-P. Chang, 1969: Spectrum analyses of large-scale wave disturbances in the tropical lower troposphere. *J. Atmos. Sci.*, **26**, 1010–1025.